



Chen, J.-J., Symes, M. D. and Cronin, L. (2018) Highly reduced and protonated aqueous solutions of [P2W18O62]6− for on-demand hydrogen generation and energy storage. *Nature Chemistry*, 10(10), pp. 1042-1047. (doi:[10.1038/s41557-018-0109-5](https://doi.org/10.1038/s41557-018-0109-5))

This is the author's final accepted version.

There may be differences between this version and the published version. You are advised to consult the publisher's version if you wish to cite from it.

<http://eprints.gla.ac.uk/166657/>

Deposited on: 14 August 2018

Enlighten – Research publications by members of the University of Glasgow
<http://eprints.gla.ac.uk>

Ultra-Reduced and Protonated Aqueous Solutions of Polyoxometalate Clusters for Flexible Energy Storage

Jia-Jia Chen, Mark D. Symes* and Leroy Cronin*

WestCHEM, School of Chemistry, the University of Glasgow, University Avenue, Glasgow G12 8QQ, UK.

Email: leroy.cronin@glasgow.ac.uk; mark.symes@glasgow.ac.uk

As our reliance on renewable energy sources grows, so too does our need to store this energy to mitigate against troughs in supply. Energy storage in batteries or by conversion to chemical fuels are the two most flexible and scalable options, but are normally considered mutually exclusive. Energy storage solutions that can act as both batteries and fuel generation devices (depending on the requirements of the user) could therefore revolutionize the up-take and use of renewably-generated energy. Herein, we present a polyoxoanion, $[\text{P}_2\text{W}_{18}\text{O}_{62}]^{6-}$, that can be reversibly reduced and protonated by 18 electrons/ H^+ per anion in aqueous solution, and which can act either as a high-performance redox flow battery electrolyte (giving a practical discharged energy density of 225 Wh L^{-1} with a theoretical energy density of more than 1000 Wh L^{-1}), or as a mediator in an electrolytic cell for the on-demand generation of hydrogen.

Our increasing reliance on renewable energy sources brings with it a need to store this energy to smooth out peaks in demand and troughs in supply.¹⁻³ Amongst the solutions proposed for this challenge, two stand out in terms of their flexibility and scalability: storage of energy as electrical charge in batteries⁴⁻⁷ and storage of energy via conversion to chemical fuels, like H_2 .⁸⁻
¹² Both approaches bring their own unique set of advantages and drawbacks, and it is often not obvious as to which would make the better choice in any given circumstance.^{13,14} Against this

background, energy storage solutions such as battery systems that can act as both batteries and fuel generation devices could have a transformative effect on how renewable energy is used.^{15,16} Soluble redox mediators are the cornerstone of these promising devices, but the electron-storage capacity of the mediators considered hitherto are limited to only 1-2 electrons per molecule. As the number of electrons that can be stored in the mediator places a fundamental limit on the energy and capacity density of these energy storage systems, there is a great need to search for new mediator systems that can store as many electrons per molecule as possible. Polyoxometalates show tremendous promise in this regard, because of their ability to store multiple electrons in a reversible manner.^{17,18} For example, Launay reported that silicotungstic acid ($[\text{H}_2\text{W}_{12}\text{O}_{40}]^{6-}$) can be highly reduced in aqueous solution,¹⁹ whilst Bond and co-workers have reported that the polyoxometalate $\alpha\text{-}[\text{S}_2\text{Mo}_{18}\text{O}_{62}]^{4-}$ is capable of taking part in extensive redox processes on the voltammetric timescale in mixed acetonitrile/water solutions.^{20,21} In many of these cases, the effects of adding protons or other small cations (*e.g.* Li^+) have been shown to be crucial for modifying the redox potentials of the polyoxometalates, facilitating the generation of reduced species at less cathodic potentials compared to when these cations are absent.²²⁻²⁴

On account of the ability of polyoxometalates to undergo a large number of redox processes in a reversible fashion, polyoxometalates have been investigated as potential energy storage devices,²⁵ including solid-state batteries (and battery electrodes) employing Li^+ ²⁶⁻³⁰ and Na^+ ^{30,31} charge carriers, and in redox flow batteries.³²⁻³⁵ In these latter cases, however, power and energy densities have hitherto been rather low, with the current champion specific energy density for a polyoxometalate-based redox flow battery being 15.4 Wh L^{-1} .³⁶ This is because polyoxometalates have not lived up to their potential in terms of storing a large number of

electrons in a reversible, and hence we hypothesised that it should be possible to produce more highly reduced systems that display reversibility.

Herein, we show that the polyoxoanion $[\text{P}_2\text{W}_{18}\text{O}_{62}]^{6-}$ displays remarkable proton-coupled-electron redox activity which allows this molecule to reversibly accept up to 18 protons and electrons in aqueous solution, allowing the construction of polyoxometalate-based redox flow batteries with energy densities of 225 Wh L^{-1} , or the rapid on-demand generation of hydrogen from water as part of a decoupled electrolysis system.

Results

The first suggestion of the extraordinary redox chemistry displayed by $[\text{P}_2\text{W}_{18}\text{O}_{62}]^{6-}$ (prepared by a modified literature procedure,³⁷ see Supplementary Sections SI-1 and SI-2 and Figure 1A) in aqueous solution was provided by cyclic voltammetry (CV) experiments in a thin layer electrochemical cell (see Figure S2-1), such as those shown in Figure 1B and 1C. Hence at a low concentration (2 mM), $[\text{P}_2\text{W}_{18}\text{O}_{62}]^{6-}$ displays four reversible waves within the range +0.6 to -0.6 V (*vs.* SHE). At pH 7, each of these waves is a simple one-electron process (black line in Figure 1B), as determined by controlled potential bulk electrolysis and by UV-vis titration, which agrees with literature reports for this compound (see Figures S2-4 to S2-6).³⁸ However, as the pH is lowered to 4, both peaks below 0 V become two-electron processes, as previously observed.³⁹⁻⁴³ Importantly, upon moving to higher concentrations of the polyoxometalate (100 mM), there is a significantly enhanced redox wave for $\text{Li}_6[\text{P}_2\text{W}_{18}\text{O}_{62}]$ below -0.3 V, when compared to the control studies at 2 mM concentration or the CV of 1 M H_2SO_4 in the absence of polyoxometalate (Figure 1C and Figure S2-7).

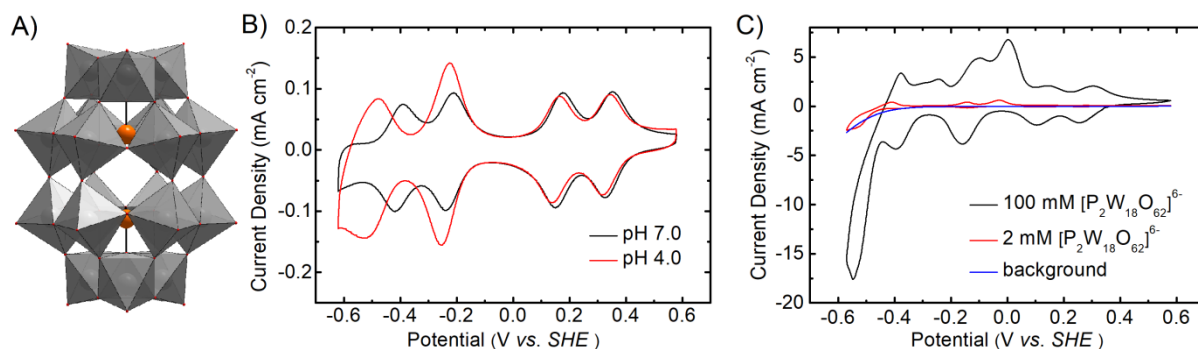


Figure 1. The structure and basic electrochemistry of $[\text{P}_2\text{W}_{18}\text{O}_{62}]^{6-}$. **A:** The structure of $[\text{P}_2\text{W}_{18}\text{O}_{62}]^{6-}$ (tungsten octahedra in grey and phosphorus in orange). **B:** CVs of a 2 mM solution of $\text{Li}_6[\text{P}_2\text{W}_{18}\text{O}_{62}]$ in 1 M Li_2SO_4 (pH 7, black line) and in 1 M $\text{Li}_2\text{SO}_4/\text{H}_2\text{SO}_4$ (pH 4, red line) at a scan rate of 10 mV s^{-1} . **C:** CVs of a 2 mM solution (red line) and 100 mM solution (black line) of $\text{Li}_6[\text{P}_2\text{W}_{18}\text{O}_{62}]$ in 1 M H_2SO_4 and a CV of just 1 M H_2SO_4 for comparison (blue line). The scan rate was 10 mV s^{-1} .

Such behaviour suggested to us that the storage of electrons in the polyoxometalate was proton-coupled, and that as the concentration of polyoxometalate in solution increased (and the pH decreased) it might be possible to store an increasing number of electrons in the polyoxometalate. Encouraged by these results, a 3-electrode electrochemical flow-cell with an Hg/HgSO_4 reference electrode was constructed to quantify the number of electrons that the polyoxometalate could store in a reversible fashion (Figure 2A, see Supplementary Information section SI-3 for details concerning the membrane,⁴⁴ materials and assembly).

In this device (Figure 2A), water was oxidised on the iridium oxide catalyst (left hand side of left hand cell), producing O_2 , protons and electrons. These electrons and protons were used to reduce and protonate an aqueous solution of $[\text{P}_2\text{W}_{18}\text{O}_{62}]^{6-}$ on the right hand side of the cell, forming more reduced polyoxoanions ($[\text{P}_2\text{W}_{18}\text{O}_{62}]^{(6+n)-}$). Once a desired amount of charge had been passed, the reduced polyoxometalate solution was then re-oxidised electrochemically by recirculation of the solution to a carbon anode in a cell like that shown on the right-hand side of Figure 2A. The charge stored reversibly in the polyoxometalate solution could then be

gauged by comparing the charge originally used to reduce the polyoxometalate with the charge obtained when it was re-oxidised.

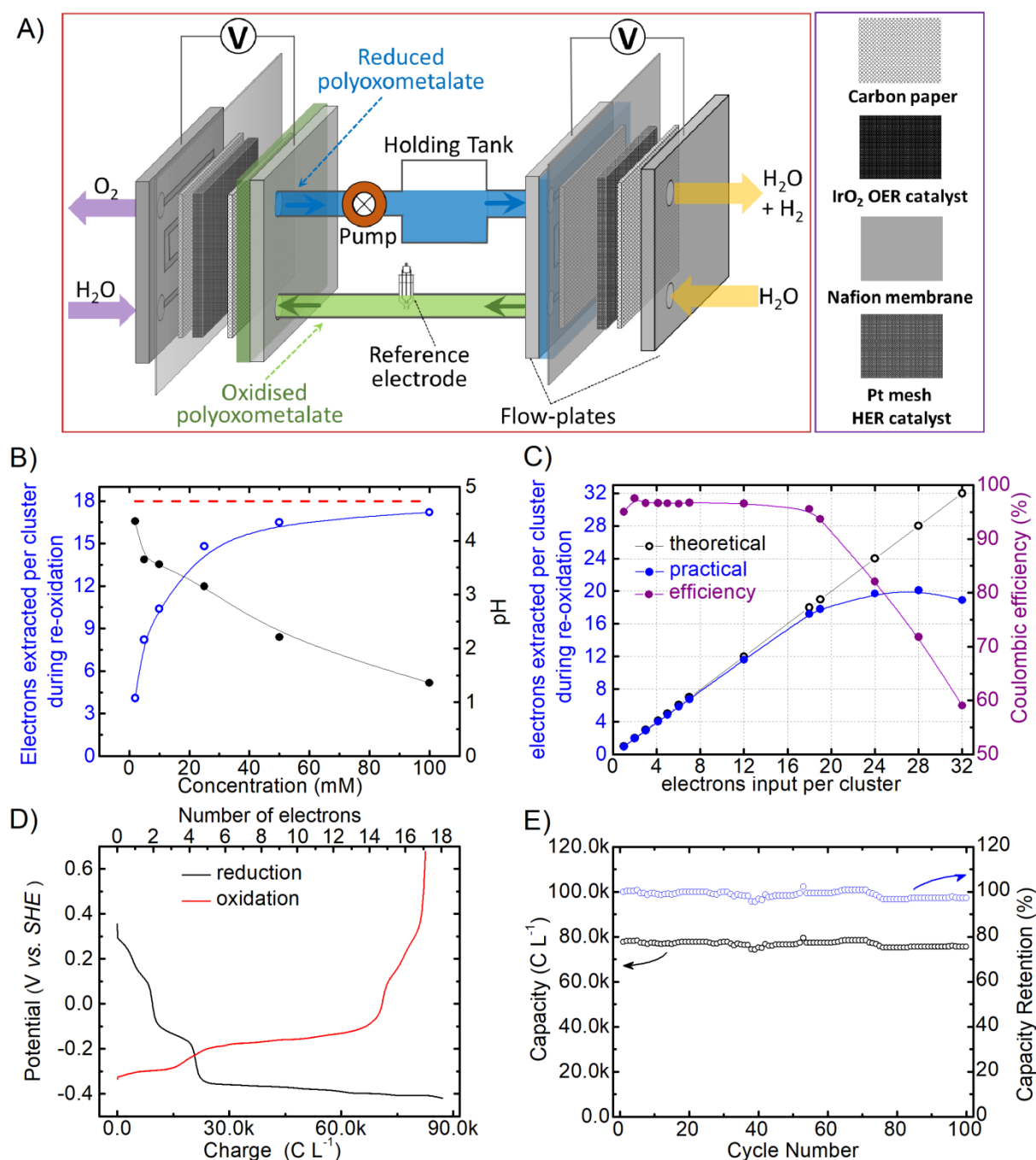


Figure 2. The reversible multi-electron redox chemistry of $[P_2W_{18}O_{62}]^{6-}$. **A:** The flow cell device used for the reduction and oxidation of $[P_2W_{18}O_{62}]^{6-}$. **B:** The relationship between polyoxometalate concentration, solution pH (measured before electro-reduction, black filled circles) and the number of electrons that can be extracted from a reduced solution of the polyoxometalate (blue open circles). The number of electrons used to reduce the polyoxometalate was limited at 18 per molecule (red dashed line). **C:** The total number of

electrons that can be extracted from a 100 mM solution of polyoxometalate after reduction by various numbers of electrons per polyoxometalate molecule. **D:** Representative 18-electron reduction/re-oxidation curves of a 50 mM solution of $[\text{P}_2\text{W}_{18}\text{O}_{62}]^{6-}$. **E:** 100 successive 18-electron reduction/re-oxidation cycles of a 50 mM solution of $[\text{P}_2\text{W}_{18}\text{O}_{62}]^{6-}$. In D and E, a current density of $\pm 50 \text{ mA cm}^{-2}$ was applied and 1 M H_2SO_4 was used as a supporting electrolyte.

The key to dramatically increasing the amount of charge in terms of protons and electrons that can be reversibly stored on the $\text{Li}_6[\text{P}_2\text{W}_{18}\text{O}_{62}]$ cluster is to increase the concentration of the cluster in aqueous solution at low pH, as shown in Figure 2B (note that these studies were conducted without any supporting electrolyte in the polyoxometalate solution). In each case, the charge passed equated to that which would be expected (in the absence of other reactions) to bring about an 18-electron reduction of the polyoxometalate (red dashed line in Figure 2B). At low polyoxometalate concentrations, it is apparent that most of the charge passed during the reduction process cannot be extracted during oxidation of the polyoxometalate solution. For example, at a concentration of cluster of 2 mM, only 4 of the 18 electrons passed during the reduction process can be recovered. By increasing the concentration of $\text{Li}_6[\text{P}_2\text{W}_{18}\text{O}_{62}]$ to 50 mM, the amount of charge recovered increased to around 16 of the 18 electrons. Analysis of the headspace of the polyoxometalate holding tank indicates that the charge that is not recovered by electrochemical re-oxidation is instead liberated as hydrogen (see Supplementary Information section SI-4). By increasing the concentration further (to 100 mM), 96% of the charge used during the reduction process can now be extracted by electrochemical re-oxidation, implying that each polyoxometalate molecule is reversibly storing an average of 17.2 electrons under these conditions (see Supplementary Information Table S3-1 and section SI-5).

Flow-cells with low ohmic polarization resistances ($\sim 20 \text{ m}\Omega$ in our case) are essential for the efficient operation of this system because the reduction of the polyoxometalate anions happens

at only slightly less cathodic potentials than hydrogen evolution (see Figure 1). Hence, we employed high flow rates of the polyoxometalate solution (100 mL min^{-1}) in order to minimize mass transport overpotentials. We also found it expedient to use galvanostatic electrolysis methods, in order to control the current density so that the polyoxometalate could be reduced without causing excessive hydrogen evolution. Using traditional static electrochemical cells (*i.e.* without any continuous flow of electrolyte) lead to much higher resistances (usually at least several dozen ohms), which were found to be too high for the polarization potential to be sufficiently controlled when using galvanostatic methods. Conversely, the use of potentiostatic methods in static electrochemical cells was found to lead to depletion of the polyoxometalate at the electrode and therefore gave rise to large hydrogen evolution currents. Hence flow-cells seem essential if excessive hydrogen evolution is to be avoided when performing the reduction of $[\text{P}_2\text{W}_{18}\text{O}_{62}]^{6-}$ by more than around 6 electrons.

The ability of the $\text{Li}_6[\text{P}_2\text{W}_{18}\text{O}_{62}]$ cluster to store large numbers electrons under flowed redox conditions was then explored by passing charge equivalent to 32 electrons per cluster at a concentration of 100 mM and measuring the difference between the reduction and oxidation process in terms of coulombic efficiency, as shown in Figure 2C (see also Figures S3-1 to S3-4). This shows that the efficiency of polyoxometalate reduction and re-oxidation remains at or above 95% up to a reduction level of 18 electrons per polyoxometalate molecule. The maximum number of electrons that can be recovered electrochemically from the reduced polyoxometalate under these conditions appears to be 20 per polyoxometalate molecule, although there are considerable parasitic losses at this maximum value. Hence, we consider 18 electrons as the maximum number of electrons that can be stored per polyoxometalate molecule under these conditions without appreciable losses to other processes.

The stability of $[\text{P}_2\text{W}_{18}\text{O}_{62}]^{6-}$ during the 18-electron redox process was probed electrochemically with successive galvanostatic reduction/re-oxidation cycles (see Figures 2D and 2E), with the coulombic efficiency of this process being $> 95\%$ with a capacity retention of 97.3% over 100 cycles. In addition, high resolution mass spectrometry analysis of a 100 mM solution of $[\text{P}_2\text{W}_{18}\text{O}_{62}]^{6-}$ after such redox cycling serves as further evidence that the polyoxometalate is stable under these conditions (see Supplementary Section SI-6).

Given that $[\text{P}_2\text{W}_{18}\text{O}_{62}]^{6-}$ can be reversibly reduced by 18 electrons with high coulombic efficiency, we decided to assess the performance of this highly-reduced polyoxometalate for proton-electron storage for on-demand hydrogen generation. Accordingly, we reduced a 100 mM solution of $[\text{P}_2\text{W}_{18}\text{O}_{62}]^{6-}$ by 18 electrons per polyoxometalate using the electrochemical flow system (left hand side of Figure 2A), and then exposed this to Pt/C (see Supplementary Section SI-7 for a description of the apparatus used). An initial rate of 3500 mmol of hydrogen per hour per mg of Pt is achieved (see Figure 3A), which is a significantly higher rate per mg of Pt than that achieved in conventional proton exchange membrane electrolyzers (where rates in state-of-the-art systems are on the order of 50 - 100 mmol of hydrogen per hour per mg of Pt).^{45,46} Figure S7-2 relates the amount of hydrogen that is evolved to the number of electrons used to reduce the polyoxometalate initially: after 400 s, around 14 of the initial 18 electrons (per polyoxometalate anion) are recovered as hydrogen, and hydrogen evolution is still ongoing (albeit at a much slower rate than initially). Given that Figure 1 shows that the final two re-oxidation potentials of the reduced polyoxometalate are anodic of the reversible hydrogen potential (0 V vs. SHE), then contact with Pt/C would only ever be expected to yield hydrogen until the two-electron reduced species was reached. Hydrogen evolution would then be expected to cease, leaving a two-electron-reduced anion, $[\text{P}_2\text{W}_{18}\text{O}_{62}]^{8-}$ (with appropriate charge-balancing cations). Hence, under these conditions, 16 is the maximum number of

electrons that can be obtained as hydrogen spontaneously by contacting the reduced polyoxometalate with Pt/C, in very good agreement with the data in Figure S7-2.

Interestingly, spontaneous hydrogen evolution from solutions of $[P_2W_{18}O_{62}]^{(n+6)-}$ can be achieved without any electrochemical bias and without the need for any catalyst, by simply diluting the solution. This is shown in Figure 3B, where 50 mM solutions of $[P_2W_{18}O_{62}]^{6-}$ (pH 2) were first reduced by 16 electrons per polyoxometalate molecule, before then being diluted to a final concentration of 2 mM with various solutions. When this dilution is carried out with water (red circles), hydrogen gas is observed to evolve spontaneously (albeit slowly) from the solution until the cluster is reduced by only 4 electrons. Meanwhile, when diluted with acidic media (50 mM H_2SO_4 and 1 M H_2SO_4 , blue and green triangles in Figure 3B respectively), the spontaneous hydrogen evolution happens much more slowly. An enhanced kinetic effect is seen when the dilution is undertaken with a non-buffering electrolyte which still allows the pH to rise (Li_2SO_4 , black diamonds). Hence raising the pH causes more rapid spontaneous hydrogen evolution during the dilution process.

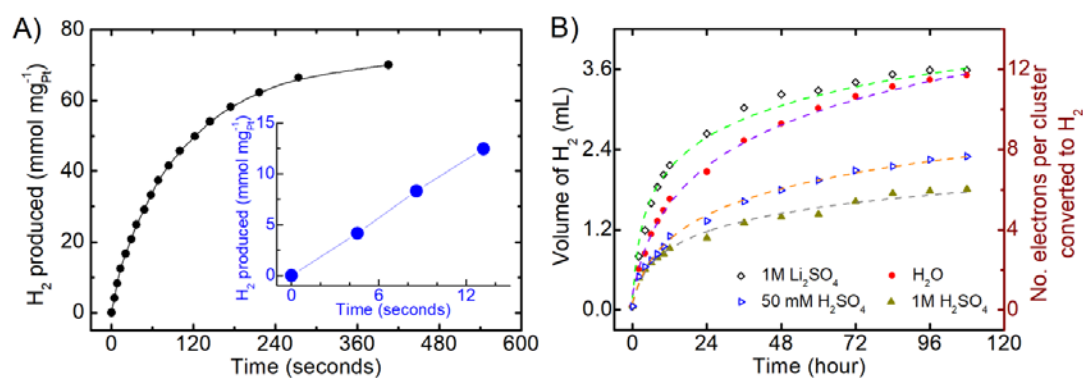


Figure 3. Hydrogen production on demand from solutions of reduced polyoxometalate. **A:** H_2 production from a 10 mL sample of 0.1 M 18-electron reduced polyoxometalate solution under an argon atmosphere in the presence of 10 mg Pt/C catalyst (1% Pt by weight). **B:** Dilution of 0.5 mL aliquots of 50 mM 18-electron reduced polyoxometalate solution with 1 M Li_2SO_4 (pH = 7), H_2O (pH = 7), 50 mM H_2SO_4 (pH = 1.5) and 1 M H_2SO_4 (pH = 1.0).

In our next set of studies exploring the extraordinary properties of the ultra-reduced $\text{Li}_6[\text{P}_2\text{W}_{18}\text{O}_{62}]$, we investigated its performance as an electrolyte in a redox flow battery. We therefore constructed a system with the cluster as the negative redox couple and using HBr/Br_2 as the positive electrolyte (see Figures 4A and 4B). A discharge capacity density of 42.6 Ah L^{-1} can be achieved at a concentration of 0.1 M at 50 mA cm^{-2} with a coulombic efficiency of 96%, as well as an energy density of 43.2 Wh L^{-1} . Upon increasing the concentration of $\text{Li}_6[\text{P}_2\text{W}_{18}\text{O}_{62}]$ to 0.3 M and 0.5 M , higher capacities of 131 Ah L^{-1} and 230 Ah L^{-1} can be achieved at $20 \text{ }^\circ\text{C}$, corresponding to practical energy densities of 130 Wh L^{-1} and 225 Wh L^{-1} respectively, see Figure 4C. Meanwhile, the energy efficiency at each of these concentrations is 76% (see Figures S9-1 to S9-3). These results are exciting since they show that this system, at the solubility limit of the cluster, would yield a flow battery with an energy density more than 1000 Wh L^{-1} , see Figure 4D. The polarization curves of this redox flow battery (Figure 4E) exhibit a peak galvanic power density of 0.52 W cm^{-2} at a concentration of $\text{Li}_6[\text{P}_2\text{W}_{18}\text{O}_{62}]$ of 0.3 M at $20 \text{ }^\circ\text{C}$, which falls off slightly at higher concentrations due to the increased viscosity of the solution. Figure 4F shows cycling data for this redox flow battery with 0.5 M $\text{Li}_6[\text{P}_2\text{W}_{18}\text{O}_{62}]$ at 0.1 A cm^{-2} within the voltage cut-offs of 0 V and 1.65 V . The galvanic discharge capacity during cycling is highly stable at around 210 Ah L^{-1} over 20 cycles with a coulombic efficiency of 98%. Cycling data using 0.1 M $\text{Li}_6[\text{P}_2\text{W}_{18}\text{O}_{62}]$ at 0.1 A cm^{-2} is shown in the Supplementary Information (Figure S9-4). Compared to current state-of-the-art negative electrolytes for redox flow batteries⁴⁷⁻⁵⁰, $\text{Li}_6[\text{P}_2\text{W}_{18}\text{O}_{62}]$ has a much higher energy density as shown in Table S9-1.

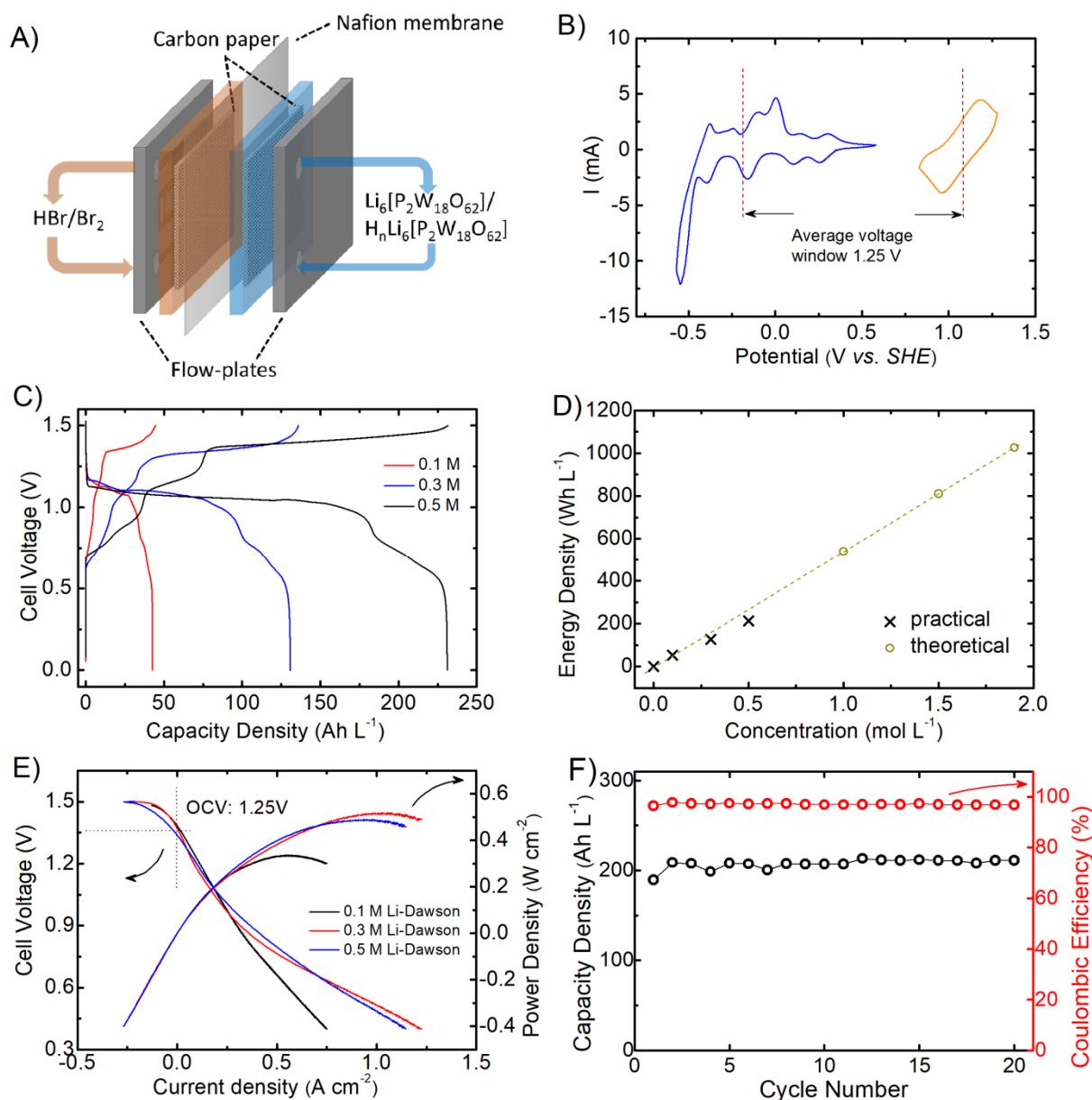


Figure 4. The application of $\text{Li}_6[\text{P}_2\text{W}_{18}\text{O}_{62}]$ in a redox flow battery. **A:** Schematic of the redox flow cell. **B:** CVs of 100 mM $\text{Li}_6[\text{P}_2\text{W}_{18}\text{O}_{62}]$ in 1 M H_2SO_4 (blue) and 0.5 M HBr in 1 M H_2SO_4 (orange) at scan rate of 10 mV s^{-1} using the setup described in Figure S2-1. **C:** Cell voltage versus capacity density with different concentrations of $\text{Li}_6[\text{P}_2\text{W}_{18}\text{O}_{62}]$ in aqueous solution on the negative side and 4 M HBr + 0.1 M Br_2 on the positive side at a current density of 50 mA cm^{-2} at $20 \text{ }^\circ\text{C}$. **D:** The relationship between energy density and concentration of $\text{Li}_6[\text{P}_2\text{W}_{18}\text{O}_{62}]$ in a redox flow battery. **E:** Polarization curves showing the power density vs. current density over the voltage range 0.4 - 1.5 V at $20 \text{ }^\circ\text{C}$ at 100% state-of-charge (OCV = open circuit voltage). **F:** Discharge capacity density and coulombic efficiency vs. cycle number obtained by applying a constant current of 0.1 A cm^{-2} over the voltage window 0 – 1.65 V at $20 \text{ }^\circ\text{C}$,

using 4 M HBr + 0.1 M Br₂ on the positive side and 0.5 M Li₆[P₂W₁₈O₆₂] in 0.1 M H₂SO₄ on the negative side.

Discussion

This work shows that polyoxometalate clusters like Li₆[P₂W₁₈O₆₂] can achieve extraordinarily effective proton-electron storage capacities in aqueous solution. This is illustrated by the ability of this cluster to accept reversibly 18 electrons and protons. This corresponds to *ca.* 9 g of hydrogen stored per litre, or a flow battery with a practical discharged energy density of 225 Wh L⁻¹ (with an open circuit voltage of 1.25 V and an energy efficiency of 76%) at room temperature at 0.5 M. Extrapolating to the limits of the solubility of this polyoxometalate (1.9 M L⁻¹ in aqueous solution), an effective storage potential of 34.2 g H₂ L⁻¹ could be achieved, which compares with pure cryogenic liquid hydrogen (71 g H₂ L⁻¹ at 20 K), and which would also yield a flow battery with an energy density breaking the 1000 Wh L⁻¹ barrier. Thus, we believe that this system will lead to new flexible energy production systems with the ability to switch between hydrogen or electrical power that could re-define the energy storage landscape. Moreover, such ultra-high capacities could transform how redox flow batteries are used, potentially allowing electric vehicles to be powered by these electrolytes.^{51,52}

Methods Summary

Supplementary Information is linked to the online version of the paper on www.nature.com/naturechemistry. This includes full experimental details for cell construction, electrochemical and mass spectrometry characterisation of the system and gas chromatography.

Acknowledgements: We thank Qi Zheng (University of Glasgow) for assistance with mass spectrometry and NMR. MDS thanks the Royal Society for a University Research Fellowship. We thank the following funders EPSRC (Grant Nos EP/H024107/1, EP/J00135X/1,

EP/J015156/1, EP/K021966/1, EP/K023004/1, EP/L023652/1), the EC (318671 MICREAGENTS), ERC (project 670467 SMART-POM).

Author Contributions: LC conceived the concept, and together LC, JJC, and MDS expanded the hypothesis, planned experiments and wrote the paper. JJC performed all the electrochemistry experiments and analysis.

Author Information Reprints and permissions information is available at www.nature.com/reprints. The authors declare no competing financial interests. Readers are welcome to comment on the online version of this article at www.nature.com/naturechemistry. Correspondence and requests for materials should be addressed to Leroy Cronin (Leroy.Cronin@glasgow.ac.uk) or Mark Symes (mark.symes@glasgow.ac.uk).

References

- 1 Dunn, B., Kamath, H. & Tarascon, J.-M. Electrical energy storage for the grid: a battery of choices. *Science* **334**, 928–935 (2011).
- 2 Cook, T. R., Dogutan, D. K., Reece, S. Y., Surendranath, Y., Teets, T. S. & Nocera, D. G. Solar Energy Supply and Storage for the Legacy and Nonlegacy Worlds. *Chem. Rev.* **110**, 6474–6502 (2010).
- 3 Roger, I., Shipman, M. A. & Symes, M. D. Earth-abundant catalysts for electrochemical and photoelectrochemical water splitting. *Nat. Rev. Chem.* **1**, 0003 (2017).
- 4 Hanley, E. S., Amarandei, G. & Glowacki, B. A. Potential of Redox Flow Batteries and Hydrogen as Integrated Storage for Decentralized Energy Systems. *Energy Fuels*, **30**, 1477–1486 (2016).
- 5 Halls, J. E. *et al.* Empowering the smart grid: can redox batteries be matched to renewable energy systems for energy storage? *Energy Environ. Sci.* **6**, 1026–1041 (2013).

- 6 Posada, J. O. G. *et al.* Aqueous batteries as grid scale energy storage solutions. *Renew. Sustainable Energy Rev.* **68**, 1174–1182 (2017).
- 7 Alotto, P., Guarnieri, M. & Moro, F. Redox flow batteries for the storage of renewable energy: A review. *Renew. Sustainable Energy Rev.* **29**, 325–335 (2014).
- 8 Olah, G. A., Prakash, G. K. S. & Goeppert, A. Anthropogenic Chemical Carbon Cycle for a Sustainable Future. *J. Am. Chem. Soc.* **133**, 12881–12898 (2011).
- 9 Le Formal, F., Bourée, W. S., Prévot, M. S. & Sivula, K. Challenges towards economic fuel generation from renewable electricity: the need for efficient electrocatalysis. *Chimia*, **69**, 789–798 (2015).
- 10 Carmo, M., Fritz, D. L., Mergel, J. & Stolten, D. A comprehensive review on PEM water electrolysis. *Int. J. Hydrogen Energy*, **38**, 4901–4934 (2013).
- 11 Symes, M. D. & Cronin, L. Decoupling hydrogen and oxygen evolution during electrolytic water splitting using an electron-coupled-proton buffer. *Nat. Chem.* **5**, 403–409 (2013).
- 12 Rausch, B., Symes, M. D., Chisholm, G. & Cronin, L. Decoupled catalytic hydrogen evolution from a molecular metal oxide redox mediator in water splitting. *Science*, **345**, 1326–1330 (2014).
- 13 Guinot, B. *et al.* Techno-economic study of a PV-hydrogen-battery hybrid system for off-grid power supply: Impact of performances' ageing on optimal system sizing and competitiveness. *Int. J. Hydrogen Energy*, **40**, 623–632 (2015).
- 14 Pellow, M. A., Emmott, C. J. M., Barnhart, C. J. & Benson, S. M. Hydrogen or batteries for grid storage? A net energy analysis. *Energy Environ. Sci.* **8**, 1938–1952 (2015).
- 15 Peljo, P. *et al.* All-vanadium dual circuit redox flow battery for renewable hydrogen generation and desulfurization. *Green Chem.* **18**, 1785–1797 (2016).

- 16 Mulder, F. M., Weninger, B. M. H., Middelkoop, J., Ooms, F. G. B. & Schreuders, H. Efficient electricity storage with a battolyser, an integrated Ni–Fe battery and electrolyser. *Energy Environ. Sci.* **10**, 756-764 (2017).
- 17 Pope, M. T. *Heteropoly and Isopoly Oxometalates*. Springer-Verlag, Heidelberg, Germany (1983).
- 18 Papaconstantinou, E. & Pope, M. T. Heteropoly Blues. III. Preparation and Stabilities of Reduced 18 –Molybdodiphosphates. *Inorg. Chem.* **6**, 1152–1155 (1967).
- 19 Launay, J. P. Reduction de l'ion metatungstate: Stades elevés de reduction de $\text{H}_2\text{W}_{12}\text{O}_{40}^{6-}$, derives de l'ion $\text{HW}_{12}\text{O}_{40}^{7-}$ et discussion generale. *J. Inorg. Nucl. Chem.* **38**, 807-16 (1976).
- 20 Way, D. M., Bond, A. M. & Wedd, A. G. Multielectron Reduction of $\alpha\text{-}[\text{S}_2\text{Mo}_{18}\text{O}_{62}]^{4-}$ in Aprotic and Protic Media: Voltammetric Studies. *Inorg. Chem.* **36**, 2826-2833 (1997).
- 21 Bond, A. M., Vu, T. & Wedd, A. G. Voltammetric studies of the interaction of the lithium cation with reduced forms of the Dawson $[\text{S}_2\text{Mo}_{18}\text{O}_{62}]^{4-}$ polyoxometalate anion. *J. Electroanal. Chem.* **494**, 96–104 (2000).
- 22 Takamoto, M., Ueda, T. & Himeno, S. Solvation effect of Li^+ on the voltammetric properties of $[\text{PMo}_{12}\text{O}_{40}]^{3-}$ in binary solvent mixtures. *J. Electroanal. Chem.* **521**, 132–136 (2002).
- 23 Grigoriev, V. A., Cheng, D., Hill, C. L. & Weinstock, I. A. Role of Alkali Metal Cation Size in the Energy and Rate of Electron Transfer to Solvent-Separated 1:1 $[(\text{M}^+)(\text{Acceptor})]$ ($\text{M}^+ = \text{Li}^+, \text{Na}^+, \text{K}^+$) Ion Pairs. *J. Am. Chem. Soc.* **123**, 5292-5307 (2001).
- 24 Ueda, T. *et al.* Voltammetric behavior of 1- and 4- $[\text{S}_2\text{VW}_{17}\text{O}_{62}]^{5-}$ in acidified acetonitrile. *Dalton Trans.* **44**, 11660-11668 (2015).

- 25 Ji, Y., Huang, L., Hu, J., Streb, C. & Song, Y.-F. Polyoxometalate-functionalized nanocarbon materials for energy conversion, energy storage and sensor systems. *Energy Environ.Sci.* **8**, 776-789 (2015).
- 26 Wang, H. *et al.* In Operando X-ray Absorption Fine Structure Studies of Polyoxometalate Molecular Cluster Batteries: Polyoxometalates as Electron Sponges. *J. Am. Chem. Soc.* **134**, 4918-4924 (2012).
- 27 Nishimoto, Y., Yokogawa, D., Yoshikawa, H., Awaga, K. & Irle, S. Super-Reduced Polyoxometalates: Excellent Molecular Cluster Battery Components and Semipermeable Molecular Capacitors. *J. Am. Chem. Soc.* **136**, 9042–9052 (2014).
- 28 Chen, J.-J. *et al.* High-Performance Polyoxometalate-Based Cathode Materials for Rechargeable Lithium-Ion Batteries. *Adv. Mater.* **27**, 4649–4654 (2015).
- 29 Huang, Q. *et al.* A highly stable polyoxometalate-based metal–organic framework with π – π stacking for enhancing lithium ion battery performance. *J. Mater. Chem. A*, **5**, 8477-8483 (2017).
- 30 Chen, J.-J. *et al.* Design and Performance of Rechargeable Sodium Ion Batteries, and Symmetrical Li-Ion Batteries with Supercapacitor-Like Power Density Based upon Polyoxovanadates. *Adv. Energy Mater.* **7**, 1701021 (2017).
- 31 Hartung, S. *et al.* Vanadium-based polyoxometalate as new material for sodium-ion battery anodes. *J. Power Sources*, **288**, 270-277 (2015).
- 32 Pratt, H. D., III, Hudak, N. S., Fang, X. & Anderson, T. M. A polyoxometalate flow battery. *J. Power Sources*, **236**, 259-264 (2013).
- 33 Pratt, H. D., III & Anderson, T. M. Mixed addenda polyoxometalate “solutions” for stationary energy storage. *Dalton Trans.* **42**, 15650-15655 (2013).
- 34 Chen, J.-J. J. & Barteau, M. A. Molybdenum polyoxometalates as active species for energy storage in non-aqueous media. *J. Energy Storage*, **13**, 255–261 (2017).

- 35 VanGelder, L. E., Kosswattaarachchi, A. M., Forrestel, P. L., Cook, T. R. & Matson, E. M. Polyoxovanadate-alkoxide clusters as multi-electron charge carriers for symmetric non-aqueous redox flow batteries. *Chem. Sci.* **9**, 1692-1699 (2018).
- 36 Liu, Y., Lu, S., Wang, H., Yang, C., Su, X. & Xiang, Y. An Aqueous Redox Flow Battery with a Tungsten–Cobalt Heteropolyacid as the Electrolyte for both the Anode and Cathode. *Adv. Energy Mater.* **7**, 1601224 (2017).
- 37 Kato, C. *et al.* Quick and selective synthesis of $\text{Li}_6[\alpha\text{-P}_2\text{W}_{18}\text{O}_{62}]\cdot 28\text{H}_2\text{O}$ soluble in various organic solvents. *Dalton Trans.* **42**, 11363-11366 (2013).
- 38 Bernardini, G., Wedd, A. G. & Bond, A. M. Reactivity of one-, two-, three- and four-electron reduced forms of $\alpha\text{-}[\text{P}_2\text{W}_{18}\text{O}_{62}]^{6-}$ generated by controlled potential electrolysis in water. *Inorg. Chim. Acta*, **374**, 327–333 (2011).
- 39 Pope, M. T. & Papaconstantinou, E. Heteropoly Blues. II. Reduction of 2:18-Tungstates. *Inorg. Chem.* **6**, 1147–1152 (1967).
- 40 Harmalkar, S. P., Leparulo, M. A. & Pope, M. T. Mixed-valence chemistry of adjacent vanadium centers in heteropolytungstate anions. I. Synthesis and electronic structures of mono-, di-, and trisubstituted derivatives of $\alpha\text{-}[\text{P}_2\text{W}_{18}\text{O}_{62}]^{6-}$. *J. Am. Chem. Soc.* **105**, 4286–4292 (1983).
- 41 Keita, B. & Nadjjo, L. New aspects of the electrochemistry of heteropolyacids part IV. Acidity dependent cyclic voltammetric behaviour of phosphotungstic and silicotungstic heteropolyanions in water and *N,N*-dimethylformamide. *J. Electroanal. Chem.* **227**, 77-98 (1987).
- 42 Prenzler, P. D., Boskovic, C., Bond, A. M. & Wedd, A. G. Coupled Electron- and Proton-Transfer Processes in the Reduction of $\alpha\text{-}[\text{P}_2\text{W}_{18}\text{O}_{62}]^{6-}$ and $\alpha\text{-}[\text{H}_2\text{W}_{12}\text{O}_{40}]^{6-}$ As Revealed by Simulation of Cyclic Voltammograms. *Anal. Chem.* **71**, 3650-3656 (1999).

- 43 Bernardini, G., Zhao, C., Wedd, A. G. & Bond, A. M. Ionic Liquid-Enhanced Photooxidation of Water Using the Polyoxometalate Anion $[P_2W_{18}O_{62}]^{6-}$ as the Sensitizer. *Inorg. Chem.* **50**, 5899–5909 (2011).
- 44 Wang, M., Zhao, F. & Dong, S. A Single Ionic Conductor Based on Nafion and Its Electrochemical Properties Used As Lithium Polymer Electrolyte. *J. Phys. Chem. B*, **108**, 1365-1370 (2004).
- 45 Millet, P. *et al.* PEM water electrolyzers: From electrocatalysis to stack development. *Int. J. Hydrogen Energy*, **35**, 5043–5052 (2010).
- 46 Xu, C., Ma, L., Li, J., Zhao, W. & Gan, Z. Synthesis and characterization of novel high-performance composite electrocatalysts for the oxygen evolution in solid polymer electrolyte (SPE) water electrolysis. *Int. J. Hydrogen Energy*, **37**, 2985–2992 (2012).
- 47 Huskinson, B. *et al.* A metal-free organic-inorganic aqueous flow battery. *Nature*, **505**, 195-198 (2014).
- 48 Lin, K. *et al.* Alkaline quinone flow battery. *Science*, **349**, 1529-1532 (2015).
- 49 Janoschka, T. *et al.* An aqueous, polymer-based redox-flow battery using non-corrosive, safe, and low-cost materials. *Nature*, **527**, 78-81 (2015).
- 50 Li, L. *et al.* A Stable Vanadium Redox-Flow Battery with High Energy Density for Large-Scale Energy Storage. *Adv. Energy Mater.* **1**, 394-400 (2011).
- 51 Mohamed, M. R., Sharkh, S. M. & Walsh, F. C. Redox flow batteries for hybrid electric vehicles: Progress and challenges. *IEEE Vehicle Power and Propulsion Conference, VPPC '09*, 551–557 (2009).
- 52 Leung, P., Li, X., Ponce de León, C., Berlouis, L., Low, C. T. J. & Walsh, F. C. Progress in redox flow batteries, remaining challenges and their applications in energy storage. *RSC Advances*, **2**, 10125–10156 (2012).